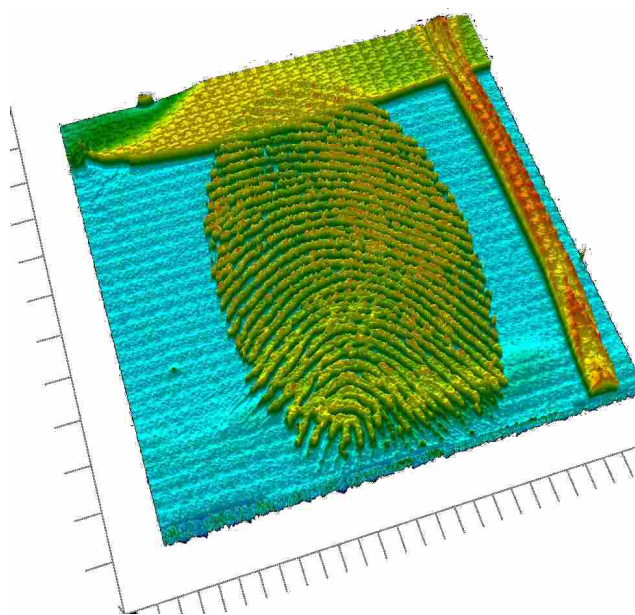


Reagents for infrared chemical imaging of fingerprints on difficult surfaces

Mark Tahtouh



A thesis submitted for the
Degree of Doctor of Philosophy (Science)
University of Technology, Sydney
May, 2008

In light of knowledge attained, the happy achievement seems almost a matter of course, and any intelligent student can grasp it without too much trouble. But the years of anxious searching in the dark, with their intense longing, their alterations of confidence and exhaustion and the final emergence into the light – only those who have experienced it can understand it.

Albert Einstein, 1933

Certificate of authorship and originality

I certify that the work in this thesis has not previously been submitted for a degree nor has it been submitted as part of the requirements for a degree except as fully acknowledged within the text.

I also certify that the thesis has been written by me. Any help that I have received in my research work and the preparation of the thesis itself has been acknowledged. In addition, I certify that all the information sources and literature used are indicated in the thesis.

Mark Tahtouh

08/12/2008

Acknowledgements

This thesis is the end product of a research project that spans several years. Over this period there have been a number of people who have contributed to the success of this project. First and foremost, I am deeply indebted to my principal supervisor Dr Brian J. Reedy. You have been the driving force behind this project since it began during my honours year (2003). You have always been supportive, encouraging and have played an enormous role in maintaining my drive and motivation. I can not thank you enough for always being helpful, supportive and encouraging throughout the highs and lows that this project has presented. You are truly the best supervisor that anyone could ask for. I am grateful to have come to know you as not only my teacher and supervisor but also as a colleague and friend.

To my co-supervisor, Dr John Kalman, I thank you for your help and support throughout this project. The organic synthetic chemistry section of this work would not have been possible without your input. I have enjoyed the many hours we have spent unlocking the mysteries of puzzling spectra and failed reactions. It has been a real pleasure and honour to work with you and I have learnt a great deal because of your involvement and enthusiasm.

To Dr Ronald Shimmon, a pseudo-supervisor, technical assistant, colleague and true friend. Your enthusiasm, commitment and helpfulness are second to none. You have made my experiences at UTS all the more enjoyable. Thanks for your help and friendship and thanks for the laughs.

To my synthetic chemistry brother, Tristan Rawling, I thank you for the laughs and good times. Thank you for never having any faith in me, my abilities or my project – you gave me motivation to prove you wrong. The organic research lab, and my experiences there, would not be complete without you. I thank you for your help and support with troublesome reactions and hereby give you credit for the 'Rawlings gamble' for improving product yield. Thank you also for your kind donation of greasy fingerprint deposits and for the gym therapy sessions that helped me through some tough times.

To my princess Kate Grimwood, thank you for being there for me and being so loving and supportive while I was being anything but. Your encouragement and patience has made more of an impact than you realise. I am happier than I have ever been because of you and I

am honoured to be walking this wonderful path through life along your side. You are my favourite and I love you. Thank you also for your greasy fingerprint deposits that, surprisingly, proved greasier than my own.

A big thank you to Pauline Despland for your help with the imaging of fingerprints on aluminium drink cans and the optimisation of parameters for FTIR chemical imaging. To Katherine Bojko (nee Flynn) for your fingerprints and help with FTIR chemical imaging. Thank you also to Dr Andrew McDonagh for helpful discussions. To Jean-Pierre Guerbois for assistance with the collection and interpretation of thermal analysis data. To Jim Keegan for assistance with GC-MS.

To all my friends, fellow students and post-graduates, past and present, thank you for your help in celebrating the good times and helping me through the bad. Whether it was sharing a laugh over lunch, a game of uno or a board meeting at the bar, you guys always helped me see there was light at the end of the tunnel. You are all, in your own way, important to me as colleagues and friends and in the interests of diplomacy, I list you here in alphabetical order: Christine Austin, Alison Beavis, David Bishop, Marty Blaber, Jessica Booth, Ellen Braybon, Adam Brown, Fiona Burger, Liz Chan, Hammish Conan, Jonathan Edgar, Matt Foot, Brad Green, Dominic Hare, Jane Hemmings, Tamsin Kelly, Ilona Kramer, Barry Lui, Katie McBean, Lisa Mingari, Julia Norman, Stephanie Notter, Sylvan Rudduck, Helen Rutledge, Joanne Salama, Garry Sarkissian, Daniel Sommerville, Sonia Taflaga, Freya Turner and Rebecca Webb.

Finally a big thank you to my family and loved ones, too numerous to list here but forever in my mind and heart. To my brothers Michael and Emil, thank you for your help and support over the past several years. You have both been helpful and a source of inspiration although you may not have realised it; I certainly did not recognise or acknowledge your importance to me often enough. To mum and dad, thank you for all your love, help and support over the past several years and indeed throughout my life. You have always done everything possible to ensure that I have the best opportunities in life and for that I am truly and humbly thankful. Your unconditional love has made me the person I am and has allowed me to pursue my dreams. Words can not express my gratitude – I love you.

Table of contents

Certificate of authorship and originality	iii
Acknowledgements	iv
Table of contents	vi
List of figures	x
List of tables	xx
Abbreviations	xxi
Abstract	xxiii
Chapter 1: Introduction	2
1.1 Fingerprints	2
1.1.1 Introduction and terminology	2
1.1.2 History of friction ridge identification	4
1.1.3 Friction ridge identification	6
1.1.4 Types of fingerprint evidence	8
1.1.5 Composition of latent fingerprints	9
1.1.6 Current fingerprint detection techniques	11
1.1.6.1 Detection techniques for porous surfaces	14
1.1.6.2 Detection techniques for non-porous surfaces	17
1.1.6.3 Detection techniques for semi-porous surfaces	25
1.1.6.4 Miscellaneous detection techniques	25
1.1.7 Difficult surfaces	26
1.1.8 Need for new fingerprint development techniques	28
1.1.9 Considerations for the preparation of fingerprint samples	29
1.2 FTIR (spectral) chemical imaging	31
1.2.1 Introduction and terminology	31

1.2.2	FTIR spectroscopy and microspectroscopy.....	35
1.2.3	FTIR mapping	35
1.2.4	FTIR chemical imaging	36
1.2.4.1	Development of FTIR chemical imaging.....	37
1.2.4.2	Forensic applications of FTIR chemical imaging	40
1.2.4.3	FTIR chemical imaging of fingerprints.....	41
1.3	Project aims	43
Chapter 2: Optimisation of parameters for infrared spectral imaging of fingerprints.....		49
2.1	Introduction	49
2.2	Materials and methods.....	51
2.3	Results and discussion	52
2.3.1	Optimisation of parameters.....	52
2.3.1.1	Spectral resolution and number of co-added scans	53
2.3.1.2	Number of image tiles (image size)	56
2.3.1.3	Spectral range and pixel aggregation	56
2.3.1.4	Image formation parameters.....	58
2.3.2	Example of optimisation of parameters – FTIR chemical imaging of fingerprints on aluminium drink cans.....	60
2.3.3	FTIR chemical imaging of fingerprints on porous surfaces	64
2.3.4	Infrared chemical imaging of large sample areas	65
2.3.4.1	Untreated Fingerprints	65
2.3.4.2	Cyanoacrylate fumed fingerprints on polymer banknotes	67
2.3.4.3	Cyanoacrylate fumed fingerprints on aluminium drink cans.....	68
2.3.5	Practical considerations and limitations of the method.....	71
Chapter 3: Synthesis of novel cyanoacrylates		74
3.1	History of cyanoacrylate synthesis	74

3.2	Cyanoacrylate monomers	78
3.3	Difficulties involved in cyanoacrylate synthesis	83
3.3.1	Patents vs journal articles	83
3.3.2	Thermal degradation of cyanoacrylates	85
3.4	Approaches to the synthesis of novel cyanoacrylates.....	91
3.4.1	Knoevenagel condensation.....	91
3.4.2	Alternative approaches.....	93
3.5	Analysis and characterisation of novel compounds	106
3.5.1	Thermal analysis of anthracene / alkyl 2-cyanoacrylate adducts.....	106
3.5.2	Nuclear magnetic resonance (NMR) spectroscopy	110
3.5.3	FTIR spectroscopy	120
3.5.4	Elemental micro analysis	125
3.6	Experimental.....	126
Chapter 4:	Use of novel cyanoacrylates for latent fingerprint enhancement.....	145
4.1	Introduction	145
4.1.1	Cyanoacrylate curing (polymerisation).....	146
4.2	Materials and methods.....	156
4.3	Results and discussion	157
4.3.1	Anthracene adducts.....	157
4.3.2	Oligo-2-cyanoethyl 2-cyanoacrylate (oligo-2-CECA).....	161
4.3.3	2-Cyanoethyl 2-cyanoacrylate (2-CECA)	162
4.3.4	1-Cyanoethyl 2-cyanoacrylate (1-CECA)	171
4.3.5	Trideuteromethyl 2-cyanoacrylate (MCA-d ₃)	179
4.3.6	Pentadeuteroethyl 2-cyanoacrylate (ECA-d ₅).....	183
4.3.7	Summary and general discussion on the use of novel cyanoacrylates for latent fingerprint enhancement.....	189

Chapter 5: Conclusions and further work.....	195
References	202

List of figures

Figure 1.1:	Classification of fingerprint patterns (from Berry and Stoney). ³	2
Figure 1.2:	Seven basic types of ridge characteristics (a) ridge ending; (b) bifurcation; (c) enclosure or lake; (d) island; (e) short ridge or dot; (f) spur or hook; (g) crossover or ridge crossing. Image adapted from Knowles and Saferstein. ^{2,5}	3
Figure 1.3:	Aging of a latent fingerprint on a porous substrate (e.g. paper) - adapted from Champod et al. ⁴	13
Figure 1.4:	Aging of a latent fingerprint on a non-porous substrate (e.g. glass) - adapted from Champod et al. ⁴	14
Figure 1.5:	Chemical reaction between ninhydrin and a primary or secondary amine that produces the dark purple product known as Ruhemann's purple (one of four resonance structures show).	15
Figure 1.6:	Structure of 1,2-indanedione.	16
Figure 1.7:	Structure of 1,8-diazafluorene-9-one (DFO).	16
Figure 1.8:	General structural formula for alkyl 2-cyanoacrylates.	18
Figure 1.9:	Structures of methyl 2-cyanoacrylate and ethyl 2-cyanoacrylate.	19
Figure 1.10:	Initiation of cyanoacrylate polymerisation – the resulting carbanion is resonance stabilised due to the presence of electron-withdrawing groups. ...	21
Figure 1.11:	Propagation of carbanion to form poly-cyanoacrylate.	21
Figure 1.12:	Cross section of polymer banknote. ⁸⁵	28
Figure 1.13:	Diagrammatic representation of 'datacube' generated by chemical imaging techniques.	34
Figure 1.14:	The approximate regions where various common types of bonds absorb (stretching vibrations only). ⁸⁸	44

Figure 1.15:	Structure of target compound: 2-cyanoethyl 2-cyanoacrylate.....	46
Figure 2.1:	Schematic showing how aluminium cans were prepared for FTIR chemical imaging.....	60
Figure 2.2:	Clamp for flattening and holding samples for subsequent FTIR chemical imaging: (a) opened position (b) top view showing sample viewing window (c) bottom view showing microscope slide used to attach clamp to motorised microscope stage.....	61
Figure 2.3:	FTIR chemical images of ethyl cyanoacrylate fumed fingerprint on aluminium drink can collected using various settings for spectral resolution and number of co-added scans: (a) Resolution 16 cm^{-1} , 64 co-added scans (b) Resolution 16 cm^{-1} , 16 co-added scans (c) Resolution 16 cm^{-1} , 4 co-added scans (d) Resolution 32 cm^{-1} , 64 co-added scans (e) Resolution 32 cm^{-1} , 16 co-added scans (f) Resolution 32 cm^{-1} , 4 co-added scans.....	62
Figure 2.4:	FTIR chemical images of ethyl cyanoacrylate fumed fingerprint on aluminium drink can collected using a pixel aggregation value of (a) 16 (pixel size $\sim 44\text{ }\mu\text{m}$) and (b) 64 (pixel size $\sim 88\text{ }\mu\text{m}$).....	63
Figure 2.5:	Untreated fingerprint on infrared reflective slide: (a) White light photograph. (b) Infrared spectrum of fingerprint residue showing peak area selected to form the FTIR chemical image (c) Monochrome representation of FTIR chemical image.....	66
Figure 2.6:	Ethyl cyanoacrylate fumed fingerprint on \$5 note (aged one month prior to fuming): (a) White light photograph. (b) Monochrome representation of FTIR chemical image.....	68
Figure 2.7:	Ethyl cyanoacrylate fumed fingerprint on Coke aluminium drink can. (a) White light photograph. (b) Monochrome representation of FTIR chemical image...	69
Figure 2.8:	Ethyl cyanoacrylate fumed fingerprint on Sprite aluminium drink can. (a) White light photograph. (b) Monochrome representation of FTIR chemical image...	70

Figure 2.9:	Ethyl cyanoacrylate fumed fingerprint on Lift aluminium drink can. (a) White light photograph. (b) Monochrome representation of FTIR chemical image... 71
Figure 3.1:	Most common route for cyanoacrylate synthesis. 75
Figure 3.2:	Initiation of cyanoacrylate polymerisation – the resulting carbanion is resonance stabilised due to the presence of electron-withdrawing groups. 76
Figure 3.3:	Propagation of carbanion to form poly-cyanoacrylate. 76
Figure 3.4:	Structures of methyl and ethyl 2-cyanoacrylate. 79
Figure 3.5:	Thermogravimetric curves of poly(ethyl α -cyanoacrylate) with various initial sample weights (W_0). Heating rate, 5 °C/min; W, transient sample weight. ²⁷⁵ 88
Figure 3.6:	Temperature of maximal rate of degradation for poly(alkyl α -cyanoacrylates) with different molecular weights (\bar{M}_n). Conditions: heating rate = 5 °C/min, initial sample weight (W_0) = 10 – 15 mg, area of polymer sample = 2 cm ² . ²⁷⁵ .. 89
Figure 3.7:	Thermogravimetric curves of poly(ethyl α -cyanoacrylate) for various quantities of H ₂ SO ₄ (acid) in the polymer sample. Conditions: heating rate = 5 °C/min, initial sample weight (W_0) = 10 mg or 60 mg, area of polymer sample = 2 cm ² . ²⁷⁵ 89
Figure 3.8:	Thermogravimetric curves of poly(ethyl α -cyanoacrylate) for various quantities of hydroquinone (radical polymerisation inhibitor) in the polymer sample. Conditions: heating rate = 5 °C/min, initial sample weight (W_0) = 10 mg or 60 mg, area of polymer sample = 2 cm ² . ²⁷⁵ 90
Figure 3.9:	Thermogravimetric curves of poly(ethyl α -cyanoacrylate) for various quantities of pyridine (base) in the polymer sample. Conditions: heating rate = 5 °C/min, initial sample weight (W_0) = 10 mg or 60 mg, area of polymer sample = 2 cm ² . ²⁷⁵ 90
Figure 3.10:	2-cyanoethyl 2-cyanoacrylate (2-CECA). 91

Figure 3.11:	Simultaneous Knoevenagel condensation and Diels-Alder 'protection' yields an anthracene / alkyl 2-cyanoacrylate adduct.....	95
Figure 3.12:	Retrograde Diels-Alder ('de-protection') of anthracene / alkyl 2-cyanoacrylate adduct yields monomeric alkyl 2-cyanoacrylate.	96
Figure 3.13:	General structural formula for alkyl bis(2-cyanoacrylate) monomers.....	97
Figure 3.14:	Reaction scheme for the synthesis of alkyl bis(2-cyanoacrylates) reported by Buck. ²³⁴	99
Figure 3.15:	Synthesis of A/CAA, A/CAC and A/CAA-K and average percentage yields obtained.	101
Figure 3.16:	Esterification reactions tested for the synthesis of A/2-CECA.	103
Figure 3.17:	Overall reaction sequence for synthesis of novel alkyl 2-cyanoacrylates.....	104
Figure 3.18:	Structures of novel anthracene / alkyl 2-cyanoacrylate adducts.....	105
Figure 3.19:	Structures of novel alkyl 2-cyanoacrylate monomers.....	105
Figure 3.20:	TGA-DTA curves for anthracene / 2-cyanoethyl 2-cyanoacrylate adduct (A/2-CECA).	107
Figure 3.21:	TGA-DTA curves for anthracene / 1-cyanoethyl 2-cyanoacrylate adduct (A/1-CECA).	108
Figure 3.22:	TGA-DTA curves for anthracene / trideuteromethyl 2-cyanoacrylate adduct (A/MCA-d ₃).	108
Figure 3.23:	TGA-DTA curves for anthracene / pentadeuteroethyl 2-cyanoacrylate adduct (A/ECA-d ₅).....	109
Figure 3.24:	General structure for Diels-Alder anthracene adducts.	112
Figure 3.25:	The four stereoisomers of anthracene / 1-cyanoethyl 2-cyanoacrylate adduct (A/1-CECA).	113

Figure 3.26:	^1H NMR spectrum of anthracene / 1-cyanoethyl 2-cyanoacrylate adduct (A/1-CECA) – resonances from residual ethanol marked with x.....	114
Figure 3.27:	^{13}C NMR spectrum of anthracene / 1-cyanoethyl 2-cyanoacrylate adduct (A/1-CECA).	115
Figure 3.28:	^1H NMR spectrum of A/1-CECA – crop 2 – resonances from residual ethanol marked with x.	116
Figure 3.29:	^{13}C NMR spectrum of A/1-CECA – crop 2.	117
Figure 3.30:	^{13}C NMR spectrum of anthracene / trideuteromethyl 2-cyanoacrylate adduct (A/MCA-d ₃) showing septet ($J_{\text{CD}} = 22.3$ Hz) for CD ₃ group at 53.2 ppm.	118
Figure 3.31:	^{13}C NMR spectrum of anthracene / pentadeuteroethyl 2-cyanoacrylate adduct (A/ECA-d ₅) showing quintet ($J_{\text{CD}}=23$ Hz) for CD ₂ group at 62.4 ppm and septet ($J_{\text{CD}}=19$ Hz) for CD ₃ group at 13.0 ppm.	119
Figure 3.32:	FTIR spectrum of anthracene / 2-cyanoacryloyl chloride adduct (A/CAC).	121
Figure 3.33:	Overlay of three FTIR spectra of A/CAC showing gradual conversion to A/CAA.	121
Figure 3.34:	FTIR spectrum of anthracene / 2-cyanoacrylic acid adduct (A/CAA).	122
Figure 3.35:	FTIR spectrum of anthracene / 2-cyanoethyl 2-cyanoacrylate adduct (A/2-CECA).	123
Figure 3.36:	FTIR spectrum of anthracene / 1-cyanoethyl 2-cyanoacrylate adduct (A/1-CECA).	123
Figure 3.37:	FTIR spectrum of anthracene / trideuteromethyl 2-cyanoacrylate adduct (A/MCA-d ₃).	124
Figure 3.38:	FTIR spectrum of anthracene / pentadeuteroethyl 2-cyanoacrylate adduct (A/ECA-d ₅).	124

Figure 4.1:	Polymerisation of cyanoacrylate with a Lewis base as the nucleophilic initiator (Nu:) forming a zwitterion, which subsequently reacts with additional monomer to form the polymer.....	147
Figure 4.2:	Raman spectra of the C≡N region (range 2290 – 2210 cm ⁻¹) showing the decrease in intensity of the band at 2235 cm ⁻¹ and the appearance of the band at 2245 cm ⁻¹ (0 hours at rear and 19 hours at front). ⁶⁶	151
Figure 4.3:	FT-Raman spectral stack-plot of ethyl 2-cyanoacrylate undergoing slow, spontaneous polymerisation. From the top: monomer at time t = 0, 7, 67, 84 and 92 days. Total time lapse of experiment, three months. Excitation at 1064 nm, wavenumber range 2300 – 2200 cm ⁻¹ showing the ν(C≡N) stretching mode near 2240 cm ⁻¹ . ⁶⁸	152
Figure 4.4:	Mid-IR transmission spectra of the curing cyanoacrylate system. Wavenumber range 2300 – 2200 cm ⁻¹ showing the ν(C≡N) stretching mode near 2240 cm ⁻¹ (only spectra recorded every minute between 0 and 5 min and finally at 100 min are displayed). ²⁹⁷	153
Figure 4.5:	Mid-IR transmission spectra of curing cyanoacrylate. Wavenumber range 2300 – 2200 cm ⁻¹ showing the ν(C≡N) stretching mode near 2240 cm ⁻¹	154
Figure 4.6:	Aluminium heating block designed to attached to soldiering iron: a) top view, b) side view, c) bottom view showing dimensions of hole for soldering iron.	159
Figure 4.7:	Custom-made cyanoacrylate fuming cabinet comprised of temperature controlled soldering iron with aluminium heat block, thermocouple for monitoring temperature, fan for circulating vapours and shelf with clips for mounting samples.	160
Figure 4.8:	Reaction vessel (one-litre) used for vacuum deposition of 2-cyanoethyl 2-cyanoacrylate.	164
Figure 4.9:	Fingerprint (donor #3) treated with 2-cyanoethyl 2-cyanoacrylate on IR reflective slide. (a) White light photograph. (b) Monochrome representation of FTIR chemical image (second derivative, 1759 cm ⁻¹). (c) Monochrome representation of FTIR chemical image (second derivative, 2252 cm ⁻¹).	166

- Figure 4.10: Fingerprint (donor #4) treated with 2-cyanoethyl 2-cyanoacrylate on IR reflective slide. (a) White light photograph. (b) Monochrome representation of FTIR chemical image (second derivative, 2252 cm^{-1})..... 167
- Figure 4.11: FTIR spectrum from ridge of fingerprint on infrared reflective slide fumed with 2-CECA (poly-2-CECA)..... 168
- Figure 4.12: Fingerprint (donor #3) treated with 2-cyanoethyl 2-cyanoacrylate on glass slide. (a) White light photograph. (b) Monochrome representation of FTIR chemical image (second derivative, 987 cm^{-1})..... 170
- Figure 4.13: Fingerprint (donor #5) treated with 1-cyanoethyl 2-cyanoacrylate on IR reflective slide. (a) White light photograph with area imaged using FTIR chemical imaging indicated. (b) Monochrome representation of FTIR chemical image (sixth derivative, 2854 cm^{-1}). 172
- Figure 4.14: FTIR spectrum from ridge of fingerprint on infrared reflective slide fumed with 1-CECA (poly-1-CECA)..... 173
- Figure 4.15: Fingerprints (donors #3 (upper) and #5 (lower)) treated with 1-cyanoethyl 2-cyanoacrylate on opaque white PMMA. (a) White light photograph with areas imaged using FTIR chemical imaging indicated. (b) Monochrome representation of FTIR chemical image (second derivative, 1774 cm^{-1}) – FTIR image has been rotated 180° relative to white light image. (c) Monochrome representation of FTIR chemical image (second derivative, 1728 cm^{-1})..... 174
- Figure 4.16: Fingerprint (donor #5) treated with 1-cyanoethyl 2-cyanoacrylate on translucent yellow fluorescent PMMA. (a) White light photograph with area imaged using FTIR chemical imaging indicated. (b) Monochrome representation of FTIR chemical image (first derivative, 1744 cm^{-1})..... 174
- Figure 4.17: Fingerprint (donor #3) treated with 1-cyanoethyl 2-cyanoacrylate on reflective gift wrap. (a) White light photograph with area imaged using FTIR chemical imaging indicated. (b) Monochrome representation of FTIR chemical image (sixth derivative, 1774 cm^{-1})..... 175

- Figure 4.18: Fingerprint (donor #5) treated with 1-cyanoethyl 2-cyanoacrylate on glossy playing card. (a) White light photograph with area imaged using FTIR chemical imaging indicated. (b) Monochrome representation of FTIR chemical image (second derivative, 1697 cm^{-1}). 175
- Figure 4.19: Image adapted from Tahtouh et al.⁷⁵ showing loss in contrast between print (fumed with conventional cyanoacrylate) and polymer banknote background on areas with raised intaglio printing. (a) White light photograph of ethyl cyanoacrylate fumed print on \$5 note. (b) Infrared spectrum of fingerprint ridge on area of banknote free from raised intaglio printing showing peak area at 1760 cm^{-1} used to generate image. (c) Infrared spectrum of area of banknote with raised intaglio printing showing increase in size and intensity of interfering background peak. (d) Monochrome representation of infrared chemical image (1760 cm^{-1} peak area). 176
- Figure 4.20: Fingerprints (donor #5) treated with 1-cyanoethyl 2-cyanoacrylate on Australian \$5 polymer banknote. (a) White light photograph with areas imaged using FTIR chemical imaging indicated. (b - e) Monochrome representations of FTIR chemical images using: (b) second derivative, 1697 cm^{-1} , (c) eighth derivative, 1682 cm^{-1} , (d) eighth derivative, 1713 cm^{-1} , (e) sixth derivative, 1713 cm^{-1} 177
- Figure 4.21: Fingerprints (donor #5) treated with 1-cyanoethyl 2-cyanoacrylate on \$5 Australian polymer banknote. (a) White light photograph with areas imaged using FTIR chemical imaging indicated. (b) Monochrome representation of FTIR chemical image (fourth derivative, 1713 cm^{-1}). (c) Monochrome representation of FTIR chemical image (fourth derivative, 1713 cm^{-1}). 178
- Figure 4.22: Fingerprint (donor #5) treated with trideuteromethyl 2-cyanoacrylate on IR reflective slide. (a) White light photograph. (b) Monochrome representation of FTIR chemical image (second derivative, 1743 cm^{-1}). 181
- Figure 4.23: FTIR spectrum from ridge of fingerprint on infrared reflective slide fumed with MCA-d₃ (poly- MCA-d₃). 182

- Figure 4.24: Fingerprints (donor #5 (a, c) and #3 (b, d)) treated with trideuteromethyl 2-cyanoacrylate on red fluorescent PMMA. (a) and (b) White light photographs with areas imaged using FTIR chemical imaging indicated. (c) Monochrome representation of FTIR chemical image of fingerprint in (a) (second derivative, 1713 cm^{-1}). (d) Monochrome representation of FTIR chemical image of fingerprint in (b) (second derivative, 1728 cm^{-1})..... 183
- Figure 4.25: Fingerprint (donor #5) treated with pentadeuteroethyl 2-cyanoacrylate on IR reflective slide. (a) White light photograph with area imaged using FTIR chemical imaging indicated. (b) Monochrome representation of FTIR chemical image (peak area 2248 cm^{-1})..... 185
- Figure 4.26: FTIR spectrum from ridge of fingerprint on infrared reflective slide fumed with ECA-d₅ (poly- ECA-d₅). 185
- Figure 4.27: Fingerprint (donor #5) treated with pentadeuteroethyl 2-cyanoacrylate on opaque white PMMA. (a) White light photograph with area imaged using FTIR chemical imaging indicated. (b) Monochrome representation of FTIR chemical image (second derivative, 1728 cm^{-1}). 186
- Figure 4.28: Fingerprint (donor #5) treated with pentadeuteroethyl 2-cyanoacrylate on glossy playing card. (a) White light photograph with area imaged using FTIR chemical imaging indicated. (b) Monochrome representation of FTIR chemical image (fourth derivative, 1651 cm^{-1})..... 187
- Figure 4.29: Fingerprint (donor #5) treated with pentadeuteroethyl 2-cyanoacrylate on Vietnamese 10,000 dong polymer banknote. (a) White light photograph with area imaged using FTIR chemical imaging indicated. (b) Monochrome representation of FTIR chemical image (peak area 2252 cm^{-1})..... 188
- Figure 4.30: Fingerprint (donor #5) treated with pentadeuteroethyl 2-cyanoacrylate on Vietnamese 10,000 dong polymer banknote. a) Monochrome representation of FTIR chemical image (peak area 2252 cm^{-1}). b) FTIR spectra from areas indicated; on fingerprint ridge (upper spectrum) and intaglio printing (lower spectrum). 189

Figure 4.31: FTIR spectrum of fingerprint treated with 2-CECA (three months after treatment)..... 191

Figure 4.32: FTIR spectrum of fingerprint treated with 2-CECA (28 months after treatment).
..... 191

List of tables

Table 1—1:	Constituents of fingerprint deposits. ^{2,4,8}	10
Table 1—2:	Types of surfaces and their interactions with latent fingerprint deposits – adapted from Champod et al. ⁴	12
Table 1—3:	Target functional groups and corresponding vibrational frequency range (stretching mode only). All vibrational frequency ranges taken from Coates ¹⁹² except for C–D stretch taken from Ley et al. ¹⁹³ and Tadokoro et al. ¹⁹⁴	45
Table 2—1:	Effect of various parameters on image collection time, file size and image quality.....	53
Table 2—2:	Typical image collection times (2.24 × 2.24 cm image) for various combinations of spectral resolution and number of co-added scans.....	54
Table 2—3:	Typical image sizes using expanded field of view optics on the Stingray FTIR imaging system.....	56
Table 2—4:	Resolution (pixel size) with variations in pixel aggregation.	57
Table 2—5:	Optimised settings for the infrared chemical imaging of cyanoacrylate-fumed fingerprints on aluminium drink cans	64
Table 3—1:	List of cyanoacrylate monomers and their boiling point.	82
Table 3—2:	Scale of reaction used from various references.....	84
Table 3—3:	Summary of thermal analysis data for anthracene / alkyl 2- cyanoacrylate adducts	110
Table 3—4:	Summary of ¹ H NMR data for several anthracene adducts.	112
Table 3—5:	Summary of chemical shift, multiplicity and coupling constants for novel deuterated compounds.....	119
Table 4—1:	Summary of fingerprints donors used during this study.....	156

Abbreviations

A/CAA	anthracene / 2-cyanoacrylic acid adduct
A/CAA-K	anthracene / 2-cyanoacrylic acid potassium salt adduct
A/CAC	anthracene / 2-cyanoacryloyl chloride adduct
A/1-CECA	anthracene / 1-cyanoethyl 2-cyanoacrylate adduct
A/2-CECA	anthracene / 2-cyanoethyl 2-cyanoacrylate adduct
A/ECA	anthracene / ethyl 2-cyanoacrylate adduct
A/ECA-d ₅	anthracene / pentadeuteroethyl 2-cyanoacrylate adduct
A/MA	anthracene / maleic anhydride adduct
A/MCA	anthracene / methyl 2-cyanoacrylate adduct
A/MCA-d ₃	anthracene / trideuteromethyl 2-cyanoacrylate adduct
ATR	attenuated total reflection
3-BPN	3-bromopropionitrile
1-CECA	1-cyanoethyl 2-cyanoacrylate
2-CECA	2-cyanoethyl 2-cyanoacrylate
2-CECAc	2-cyanoethyl cyanoacetate
DAB	diaminobenzidine
DBU	1,8-diazobicyclo[5,4,0]undec-7-ene
DFO	1,8-diazafluorene-9-one
DMAC	dimethylaminocinnamaldehyde
DMF	<i>N,N</i> -dimethylformamide
DMSO	dimethylsulfoxide
DTA	differential thermal analysis
ECA	ethyl 2-cyanoacrylate (superglue)
ECA-d ₅	pentadeuteroethyl 2-cyanoacrylate
FPA	focal plane array
FTIR	Fourier transform infrared
GS-MS	gas chromatography – mass spectrometry
HSAB	hard soft acid base
HMPA	hexamethylphosphoramide
3-HPN	3-hydroxypropionitrile
2-HPN	2-hydroxypropionitrile
IR	infrared

MCA-d ₃	trideuteromethyl 2-cyanoacrylate
MMD	multi-metal deposition
MNF	minimal noise fraction
MS	mass spectrometry
NMR	nuclear magnetic resonance
NWSD	non-water-soluble deposit
oligo-2-CECA	oligo-2-cyanoethyl 2-cyanoacrylate
OsO ₄	osmium tetroxide
PD	physical developer
PC	principal component
P ₂ O ₅	phosphorus pentoxide
poly-1-CECA	1-cyanoethyl 2-cyanoacrylate polymer
poly-2-CECA	2-cyanoethyl 2-cyanoacrylate polymer
poly-ECA-d ₅	pentadeuteroethyl 2-cyanoacrylate polymer
poly-MCA-d ₃	trideuteromethyl 2-cyanoacrylate polymer
RTX	ruthenium tetroxide
SO ₂	sulfur dioxide
SOCl ₂	thionyl chloride
SPR	small particle reagent
TGA	thermogravimetric analysis
VMD	vacuum metal deposition
WSD	water-soluble deposit

Note: as a supplement to the above list of abbreviations, a fold out page at the back of this thesis contains structures, names and abbreviations for the majority of the compounds discussed.

Abstract

Fingerprints continue to be an important form of forensic evidence for individual identification. A number of techniques are currently available for the detection and enhancement of invisible or latent fingerprints. While these techniques perform well on many surfaces, there are a number of surfaces that pose problems. On such surfaces, Fourier transform infrared (FTIR) chemical imaging can provide superior results. FTIR chemical imaging involves the simultaneous collection of thousands of mid-infrared spectra across a sample using a focal plane array (FPA) detector. This allows for the collection of chemically specific spectral data while maintaining spatial information. Images can then be generated based on spectral / chemical contrast between components within a sample. A key aim of this project was to further investigate the use of FTIR chemical imaging for the detection and enhancement of latent (untreated) and developed (treated) fingerprints on a number of 'difficult' surfaces.

During the initial development of an infrared chemical imaging technique for fingerprints, an un-optimised set of image collection parameters was used. Using these settings, the collection of an entire fingerprint image was time consuming (often several hours or days). A systematic method for the optimisation of the image collection parameters has been developed. This method allows the optimisation of parameters such as spectral resolution, number of co-added scans, spectral range, pixel aggregation and image formation parameters in order to minimise image collection time and file size while maintaining the quality of the fingerprint image produced.

A commonly-used fingerprint detection technique for latent fingerprints on non-porous or semi-porous surfaces involves fuming samples with monomeric ethyl 2-cyanoacrylate (superglue). This reagent leaves a white residue (polymeric cyanoacrylate) on the ridges of latent fingerprints, rendering them visible under white light. On some surfaces, such as polymer banknotes, however, the contrast between cyanoacrylate-developed fingerprints and the background is poor. FTIR chemical imaging of cyanoacrylate fumed fingerprints on polymer banknotes and other difficult surfaces has been shown to provide better results than optical techniques alone. During this project, further investigations into the use of FTIR chemical imaging for latent fingerprints treated with commercial cyanoacrylate monomer on a range of difficult surfaces were conducted. While excellent results were obtained on many

samples, the need for novel cyanoacrylates containing infrared absorbance in specific parts of the spectrum was identified.

A major focus of this project has been the identification, synthesis and characterisation of modified cyanoacrylates which may be used as reagents for FTIR chemical imaging of fingerprints. Monomers that contained particular functional groups that show vibrational modes in the range from 2500 – 1800 cm^{-1} were sought. This region typically contains very few vibrational bands and therefore a reagent that could be used to give fingerprints absorptions in this range is desirable. This would provide the necessary contrast between the ridge details of the treated fingerprint and the background on which it may be located.

In total four novel cyanoacrylates were prepared. These included 2-cyanoethyl 2-cyanoacrylate (2-CECA), 1-cyanoethyl 2-cyanoacrylate (1-CECA), trideuteromethyl 2-cyanoacrylate (MCA-d₃) and pentadeuteroethyl 2-cyanoacrylate (ECA-d₅).

Each of the four novel monomers was tested a reagent for the detection and enhancement of latent fingerprints on a number of surfaces via FTIR chemical imaging. The 2-CECA monomer was found to be less volatile than conventional cyanoacrylate and thermally decomposed at the temperatures required to vaporise it. Treating latent fingerprints with this monomer at a reduced pressure yielded better results on reflective surfaces. On less reflective surfaces, such as polymer banknotes, however, the nitrile band of 2-CECA was almost undetectable and therefore could not be used for imaging the treated prints.

Fingerprints treated with the deuterated monomers (MCA-d₃ and ECA-d₅) showed characteristic bands in the region from 2300 – 1900 cm^{-1} owing to C–D stretching vibrations. Once again, however, the relatively low intensity of these bands meant that they were only detected from prints on reflective surfaces.

The monomer that produced the best results was 1-CECA. Surprisingly the contrast between the ridge detail and the background, was not generated by the nitrile band at 2250 cm^{-1} as anticipated. Instead it appears that the absorption band for the carbonyl group in poly-1-CECA is sufficiently resolved from any absorption within this region from the background surface (such as polymer banknotes) to provide good contrast images of the treated fingerprint. High quality fingerprint images were obtained of prints treated with 1-CECA on

all difficult surfaces tested including white opaque acrylic sheets, fluorescent acrylic sheets and all areas of polymer banknotes including areas containing raised intaglio printing.